MICROCOPY RESOLUTION TEST CHART

NATIONAL BUREAU OF STANDARDS-1963-A

SECURITY CLASSIFICATION OF THIS PAGE *(When Data Entered)*

REPORT DOCUMENTATION PAGE		READ INSTRUCTIONS BEFORE COMPLETING FORM
1. REPORT NUMBER AFOSR·TR· 86-0565	2. GOVT ACCESSION NO.	3. RECIPIENT'S CATALOG NUMBER
4. TITLE *(and Subtitle)* Radiative Energy Transfer and Thermal Management in Advanced Space Power and Propulsion Systems		5. TYPE OF REPORT & PERIOD COVERED Annual Report, 1 OCT. 1983 – 30 SEPT. 1984
		6. PERFORMING ORG. REPORT NUMBER
7. AUTHOR(s) A. T. Mattick and A. Hertzberg		8. CONTRACT OR GRANT NUMBER(s) AFOSR-83-0367
9. PERFORMING ORGANIZATION NAME AND ADDRESS University of Washington Seattle, WA 98195		10. PROGRAM ELEMENT, PROJECT, TASK AREA & WORK UNIT NUMBERS 61102F 2301/K2
11. CONTROLLING OFFICE NAME AND ADDRESS Aerospace & Energetics Research Program		12. REPORT DATE March 4, 1986
		13. NUMBER OF PAGES 22
14. MONITORING AGENCY NAME & ADDRESS(if different from Controlling Office) Air Force Office of Scientific Research Bolling AFB, D.C. 20332		15. SECURITY CLASS. (of this report) Unclassified
		15a. DECLASSIFICATION/DOWNGRADING SCHEDULE

16. DISTRIBUTION STATEMENT *(of this Report)*

N/A

Approved for public release, distribution unlimited

17. DISTRIBUTION STATEMENT *(of the abstract entered in Block 20, if different from Report)*

N/A

DTIC
ELECTE
AUG 1 2 1986
B

18. SUPPLEMENTARY NOTES

N/A

19. KEY WORDS *(Continue on reverse side if necessary and identify by block number)*

20. ABSTRACT *(Continue on reverse side if necessary and identify by block number)*

Technical results for the first year of research on AFOSR grant 83-0367 are summarized. This work involved a theoretical study of radiation transfer in droplet clouds, for predicting the performance of the liquid droplet radiator. The effects on droplet sheet emissivity of non-isotropic scattering by droplets and of the development of a temperature profile on the droplet sheet are shown to be small.

DD FORM 1473 EDITION OF 1 NOV 65 IS OBSOLETE
1 JAN 73

Unclassified
SECURITY CLASSIFICATION OF THIS PAGE *(When Data Entered)*

86 8 8 072

AFOSR·TR· 86-0585

Annual Report - AFOSR Grant   83-0367

Research Period: 1 Oct. 1983 - 30 Sept. 1984

A.T. Mattick and A. Hertzberg

Abstract

Technical results for the first year of research on AFOSR grant 83-0367 are summarized. This work involved a theoretical study of radiation transfer in droplet clouds, for predicting the performance of the liquid droplet radiator. The effects on droplet sheet emissivity of non-isotropic scattering by droplets and of the development of a temperature profile on the droplet sheet are shown to be small.

1. Introduction

This report summarizes the results of a theoretical analysis of radiation transfer in droplet clouds carried out during the period 1 Oct. 1983 to 30 Sept. 1984 on AFOSR grant 83-0367. This program of research was initiated to establish a theoretical foundation for predicting the performance of the liquid droplet radiator (LDR), an advanced heat rejecttion system for space power. A schematic of the baseline configuration for this radiation is shown in Fig. 1. Waste heat is transferred to a liquid, which is sprayed into space in the form of submillimeter droplets. The droplet trajectories must be controlled accurately enough that all the liquid can be collected, once the droplets have cooled by radiating their energy to space. This concept has the promise of being much lighter than conventional radiator designs which use solid surfaces to reject waste heat.

Previous analyses of the radiation by the rectangular sheet of droplets carried out by the investigators[1,2], had assumed that the temperature did not vary in the sheet thickness direction and that the droplets scattered radiation isotropically. The chief aims of the present program were to derive a formalism for radiative transfer in an LDR droplet sheet which included the effects of non-isotropic scattering and a time dependent temperature profile, and to find numerical solutions for the droplet sheet emissivity. The investigators have accomplished these goals during the first year of the program, and have initiated an experimental program to test the predictions of the theory, by measuring the radiation emitted by a cloud of droplets.

The theoretical analysis of radiation transfer including non-isotropic scattering indicated that for droplet sheet parameters of interest for the LDR, non-isotropic and isotropic results do not differ substantially. Likewise allowance for a non-uniform temperature profile in the sheet thickness direction has only a small effect on the power emitted by an LDR droplet sheet.

Investigation of a solar thermophotovoltaic system for space power was terminated because an engineering analysis of the liquid silicon storage scheme for this system indicated that materials incompatibility problems are insurmountable. Another research area of the proposal for this grant was the investigation of the emissive properties of metals and alloys, along with investigation of methods for increasing emissivities of low emissivity materials which otherwise have promise as candidate LDR fluids. We carried out a literature survey of the emissive properties of metals, both to find optical characteristics of classes of metals and to find a suitable theory for predicting emissivities of metal mixtures. This extensive survey revealed that the existing data on metal emissivities (particularly for tin and tin alloys, and for alkali metals) was very scarce, particularly for the liquid phase, and secondly, that there is at present no theory of metal emissivity which can acccurately predict the temperature dependence of emissivity. We concluded that further efforts in this area, either in measuring liquid metal emissivities, or in making fundamental contributions in the theory of optical properties of metals, was beyond the scope of the program.

2. Analysis of Radiation Transfer in Droplet Clouds

The purpose of the theoretical program was to develop a more complete model of radiation transfer in droplet clouds used for the liquid droplet radiator (LDR) than had previously been used. Our prior work on this problem had assumed a simple model of an LDR droplet sheet in which the droplet temperature was uniform and in which scattering of radiation by droplets was isotropic.[1,2] The radiation interaction with the droplets was treated using geometrical optics. The principal modifications to this model addressed in the present program were the allowance for a non-uniform temperature profile and for non-isotropic scattering by the droplets. Our goal was to determine the effects these phenomena would have on the radiative characteristics of a droplet sheet as compared to the results from our simple model.

Model of a Planar LDR Droplet Sheet

In the baseline configuration of the liquid droplet radiator (Fig. 1.) a rectangular array of heated liquid droplets is ejected into space at the droplet generator. The width W of this array (y-direction) is generally much larger than the thickness S (x direction): The droplets traverse a distance L (sheet length, z direction), radiating waste heat into a radiation vacuum (no incident radiation).

The droplet sheet is analogous to a solid radiating surface of a conventional radiator, and it is conveniently characterized by a hemispherical emissivity ϵ_s from its "surfaces," which are the top and bottom of a rectangular sheet and have dimensions W×L. Generally W and L are of comparable magnitude and the area, WL, is chosen to meet the heat rejection requirements of a specific application, i.e., $P_{rad} = 2\epsilon_s \sigma_B T^4 WL$,

where σ_B is the Stefan-Boltzmann constant. The sheet emissivity ϵ_s may vary with distance z along the direction of droplet propagation. The sheet emissivity depends on the number density of droplets and sheet thickness, which are assumed constant along the sheet length, and also on the absorption and scattering properties of individual droplets which may in turn depend on temperature. The variation in sheet emissivity thus arises from a decrease in the mean temperature of the droplets (in an x-y slice through the sheet) as they traverse the transit length L, and also from the development of a temperature profile through the thickness of the sheet (x-direction). Although the droplets have a uniform temperature as they are ejected into space, a temperature variation in the thickness direction will develop because the droplets nearer the surfaces will cool faster than interior droplets.

Our analytical model of radiation transfer in a droplet sheet makes two simplifying assumptions based on the relative sheet dimensions. The sheet thickness S is chosen so that the optical depth $\tau_{ox} \equiv n\sigma S$ of the sheet in the thickness direction will be of order unity. (n is the number density of droplets and $\sigma = \pi a^2$ is the frontal area of a droplet.) For practical designs (see Ref 3) this dimension will be on the order of centimeters, whereas the dimensions W and L will be on the order of 10's of meters. Edge effects will be important only over distances corresponding to ~1 optical depth. Thus variation of temperature in the y-direction (sheet width) will only be significant over a fraction ~0.001 of the sheet width. Our first assumption, then, is that the sheet is effectively infinitely wide, and there is no variation of droplet temperature or radiation intensity in the y-direction. A second simplification arises from the fact that S/L <<< 1 and that for a practical LDR design the fractional temperature decrease of

droplets in flight is $\lesssim 0.5$. The logarithmic derivative of temperature with optical depth along the z direction is

$$\frac{1}{T}\frac{\partial T}{\partial \tau_z} \sim \frac{\Delta T/T}{\tau_{oz}} = \frac{\Delta T/T}{\tau_{ox}}\frac{S}{L}$$

and is of order 10^{-3}.

Droplets at a given point in the sheet only interact radiatively with those within an optical distance of order unity. Since the fractional variation in droplet temperature (and droplet radiation) over one optical depth in the z direction is extremely small, we neglect it. The second assumption, then, is that the temperature is uniform in the z-direction. The two assumptions reduce the model to a single dimension, x, and the problem is to determine the temperature evolution of an infinite slab of radiating droplets, which initially have a uniform temperature. This infinite slab represents a slice of the droplet sheet as it propagates from the droplet generator to the collector. The above considerations assure that this model will predict the radiative characteristics of an LDR droplet sheet (finite W and L) very precisely.

Radiative Transfer Equations

In the model described above, the infinite droplet sheet will have a uniform initial temperature, but since the droplets nearer the surface of the sheet cool more rapidly than interior droplets a non-uniform temperature profile will evolve normal to the sheet, i.e., $T = T(x,t)$. It is nonetheless useful to characterize the sheet by a hemispherical sheet emissivity based on the average sheet temperature:

$$\overline{T}(t) = \frac{1}{S}\int_0^S dx\ T(x,t)\ . \tag{1}$$

The sheet emissivity is defined to be:

$$\epsilon_S(t) \equiv J(t)/\sigma_B \overline{T}^4(t) \tag{2}$$

where $J(t)$ is the hemispherical power/unit area emitted by a surface of the
sheet. This convention is useful because the energy balance equation then
has the same form as that for a uniform temperature system:

$$m_S C \frac{d\overline{T}}{dt} = 2\epsilon_S \sigma_B \overline{T}^4 \quad , \tag{3}$$

where m_S is the fluid mass/(projected sheet area), and C is the specific
heat of the fluid. The principal aims of our program were to determine the
time evolution of ϵ_S and to evaluate the effect of non-isotropic scattering
on ϵ_S. When considering fluids which exhibit structure in their absorption
and emission spectra, and also for the spectral variation in droplet
scattering due to wave effects, it is often necessary to consider the
spectral sheet emissivity

$$\epsilon_{S\nu}(t) = J_\nu(t)/J_\nu^B(\overline{T})$$

where J_ν is the sheet hemispherical intensity/(unit frequency), and $J_\nu^B(t)$ is
the blackbody hemispherical intensity/(unit frequency):

$$J_\nu^B(\overline{T}) = \frac{h}{c^2} \nu^3/(\exp(h\nu/k\overline{T})-1) \quad .$$

The relationship between $\epsilon_{S\nu}$ and ϵ_S is given by:

$$\varepsilon_S = \int d\nu \varepsilon_{S\nu} J_\nu^B / \sigma_B \overline{T}^4 \tag{4}$$

and, of course,

$$J(t) = \int d\nu J_\nu(t)$$

$$\sigma_B T^4 = \int d\nu J_\nu^B(T) \quad .$$

The droplet temperature is governed by the equation of radiative transfer:

$$\frac{\partial I_\nu(x,\Omega,t)}{\partial x} \cos\theta = n\sigma \ \{- I_\nu(x,\Omega,t)(\varepsilon_{0\nu} + \omega_\nu)$$

$$+ \varepsilon_{0\nu} J_\nu^B[T(x,t)]/\pi$$

$$+ \frac{\omega_\nu}{4\pi} \int d\Omega' I_\nu(x,\Omega',t)\sigma_\nu(\Omega' \to \Omega)\} \tag{5}$$

and by radiative energy balance for a droplet:

$$mC \ \frac{\partial T(x,t)}{\partial t} = \int d\nu \ \{-4\sigma \ \varepsilon_{0\nu} J_\nu^B[T(x,t)]$$

$$+ \varepsilon_{0\nu} \sigma \int d\Omega \ I_\nu(x,\Omega,t)\} \quad . \tag{6}$$

In these equations, n is the number density of droplets, m is the droplet mass, C is the fluid specific heat, $\sigma = \pi a^2$ is the projected geometrical cross-section of a droplet (a = droplet radius), $\varepsilon_{0\nu}$ is the frequency-dependent droplet emittance (often called the absorption efficiency) and ω_ν is the scattering efficiency. Note that the total scattering and absorption cross-sections at frequency ν are $\sigma\omega_\nu$ and $\sigma\varepsilon_{0\nu}$, respectively. The spectral

intensity per solid angle, $I_\nu(x,\Omega,t)$, in droplet sheet is not only a function of frequency, position and time, but also of direction $\Omega = (\theta,\psi)$ where θ is the polar angle from the sheet normal $\hat{x}$, and ψ is the azimuthal angle. In fact, I_ν is independent of ψ due to the symmetry of the problem. The non-isotropy of scattering is expressed by the phase function ϕ_ν which is normalized to 4π, i.e., $\int d\Omega' \phi(\Omega' \to \Omega) = 4\pi$. (For isotropic scattering $\phi_\nu = 1$.) The quantities $\epsilon_{0\nu}$, ω_ν, and ϕ_ν can be obtained from the Mie scattering theory if the complex index of refraction, $n = n_1 + in_2$, is known as a function of frequency. These quantities are generally complicated functions of the size parameter $z = 2\pi a/\lambda$. For droplets which are large compared to the radiation wavelength ($z \gtrsim 100$) the scattering exhibits very rapid oscillations as a function of scattering angle and a very strong peak over a narrow range of angles in the forward direction. However, if averaged over a small range of frequencies (or equivalently, z), the scattering is very nearly isotropic, aside from the forward peak. This peak can be subtracted from the scattering distribution because, for the present problem, forward scattered light does not differ from transmitted light. For smaller values of z, the non-isotropy varies more slowly with angle and cannot be "averaged out." In fact, an average of ϕ over a range of wavelengths large enough to incorporate 2 or more nodes, still yields a non-isotropic distribution. This fact was the primary basis for our investigation of the effects of non-isotropic scattering on droplet sheet emissivity.

Owing to the symmetry of the problem about a pane midway through the sheet (at $x = S/2$), we have $(I_\nu(x,\theta>\frac{\pi}{2},t) = I_\nu(S-x,\pi-\theta,t)$. The formalism is also simplified if we change from independent variable x to a new variable $\tilde{\tau}_\nu$ defined below, and introduce the relative efficiencies $\tilde{\epsilon}_{0\nu}$, $\tilde{\omega}_{0\nu}$:

$$\tilde{\tau}_\nu = n\sigma x(\varepsilon_{0\nu}+\omega_\nu) = \tau(\varepsilon_{0\nu}+\omega_\nu)$$

$$\tilde{\varepsilon}_{0\nu} = \varepsilon_{0\nu}/(\varepsilon_{0\nu}+\omega_\nu) \tag{7}$$

$$\tilde{\omega}_\nu = \omega_\nu/(\varepsilon_{0\nu}+\omega_\nu) \quad .$$

For convenience the tilde will be omitted below. We can formally integrate eq. (5), to obtain:

$$I_\nu(\tau_\nu,\theta,t) = \frac{1}{\cos\theta} \int_0^\tau d\tau_\nu' \exp\left[- \frac{\tau_\nu-\tau_\nu'}{\cos\theta}\right] \cdot \{\varepsilon_{0\nu}J_\nu^B[T(\tau_\nu',t)]/\pi \tag{8}$$

$$+ \omega_\nu\int_0^{\pi/2} d\theta'\sin\theta' [I_\nu(\tau_\nu',\theta',t)\gamma^+(\theta,\theta')+I_\nu(\tau_{0\nu}-\tau_\nu',\theta',t)\gamma^-(\theta,\theta')]\}$$

$$\text{where} \quad \gamma^\pm(\theta,\theta') = \frac{1}{4\pi} \int_0^{2\pi} d\psi \left\{ \begin{array}{c} \sigma_\nu(\theta,0;\theta',\psi) \\ \\ \phi_\nu(\theta,0;\pi-\theta',\psi) \end{array} \right. \quad .$$

In order to isolate the effects of a nonuniform temperature profile and non-isotropic scattering on droplet sheet emissivity, simplified approaches will be taken – isotropic scattering was assumed in determining the evolution of a temperature profile, and a uniform temperature was assumed in determining the effects of non-isotropic scattering. We shall describe the analysis of each case separately.

Temperature Profile of a Droplet Sheet

In the determination of the temperature profile of a droplet sheet, we assume isotropic scattering, so that $\phi_\nu = 1$ and $\gamma^-=\gamma^+=1/2$. We further assume that the droplets are gray bodies, that is, the scattering and absorption efficiencies have no frequency dependence. With these

assumptions we can immediately integrate eq. (8) over frequency, and carry out the frequency integral in eq. (6) to obtain:

$$I(\tau,\mu,t) = \frac{1}{\mu} \int_0^\tau d\tau' \exp\left[-\frac{\tau-\tau'}{\mu}\right] \cdot \{\varepsilon_0 \sigma_B T^4(\tau',t)/\pi$$

$$+ \frac{\omega}{2} \int_0^1 d\mu'[I(\tau',\mu',t)+I(\tau_0-\tau',\mu',t)]\} \tag{9}$$

$$mC \frac{\partial T(\tau,t)}{\partial t} = -4\varepsilon_0 \sigma \sigma_B T^4(\tau,t)$$

$$+ 2\pi\varepsilon_0 \sigma \int_0^1 d\mu[I(\tau,\mu,t) + I(\tau_0-\tau,\mu,t)] \tag{10}$$

where $\mu = \cos\theta$. Denoting the quantity in curly braces by $\tilde{f}(\tau',t)$, introducing a dimensionless variable $f(\tau,t) = \tilde{f}(\tau,t)\cdot(\pi/\varepsilon_0\sigma_B T_0^4)$, where T_0 is the initial temperature, and also using a reduced temperature $\tilde{T} \equiv T/T_0$, we obtain:

$$f(\tilde{\tau},\tilde{t}) = \tilde{T}^4(\tilde{\tau},\tilde{t}) + \frac{\tilde{\omega}}{2} \int_0^{\tilde{\tau}_0} d\tilde{\tau}' \, E_1(\,\tilde{\tau}-\tilde{\tau}'\,)f(\tilde{\tau}',\tilde{t}) \tag{11}$$

$$\frac{\partial \tilde{T}(\tilde{\tau},\tilde{t})}{\partial \tilde{t}} = -\tilde{T}^4(\tilde{\tau},\tilde{t}) + \tilde{\varepsilon}_0 f(\tilde{\tau},\tilde{t}) \tag{12}$$

where the time variable has been replaced by the dimensionless quantity:

$$\tilde{t} = t \, 4\tilde{\varepsilon}_0\sigma\sigma_B T_0^3/mC\tilde{\omega} \tag{13}$$

and we have reincorporated the tildes for the quantities τ, ω, and ε_0. $E_n(x)$ is the exponential integral $\int_1^\infty dz \, e^{-xz}/z^n$.

The coupled equations 11 and 12 are to be solved to obtain the temperature profile $\tilde{T}(\tau,\tilde{t})$, with the initial condition $\tilde{T}(\tau,0) = 1$. The solution parameters are the modified optical depth $\tilde{\tau}_0 = \tau_0(\epsilon_0+2)$ and the modified droplet emittance $\tilde{\epsilon}_0 = \epsilon_0/(\epsilon_0+\omega)$, since $\tilde{\omega} = 1-\tilde{\epsilon}_0$. For large droplets $\epsilon_0+\omega = 1$, so that $\tilde{\tau}=\tau$ and $\tilde{\epsilon}_0 = \epsilon_0$. Assuming this to be the case, we can again drop the tilde notation. The hemispherical emissivity of the droplet sheet is:

$$\epsilon_S(\tilde{t}) = \int_0^1 \mu d\mu \ I(\tau_0,\mu,\tilde{t})/\sigma_B \overline{T}^4(\tilde{t})$$

or

$$\epsilon_S = \frac{\epsilon_0}{\pi} \int_0^{\tau_0} d\tau \ E_2(\tau)f(\tau,\tilde{t})/\overline{T}^4(t) \quad . \tag{14}$$

Equations 11 and 12 were solved in an iterative fashion. The intensity function f was determined for a given distribution $\tilde{T}$ by solving integral equation 11 numerically. The approach was similar to that used in our earlier, uniform temperature calculations where the half sheet (since the problem is symmetrical) was broken up into individual stations. The integral equation was then transformed into a matrix equation:

$$f_i(\tilde{t}) = \tilde{T}_i^4(\tilde{t}) + \frac{\omega}{2} \sum_j A_{ij} f_j(\tilde{t}) \tag{15}$$

and f could be determined by a simple matrix inversion. The distribution $f_i(\tilde{t})$ was then used as a source function to advance $\tilde{T}_i(\tilde{t})$ by a small time increment $\Delta\tilde{t}$ using eq. (12).

Numerical solutions for the temperature profile as a function of time were obtained for a wide range of optical depths and droplet emittances. From an initial state of uniform temperature there is a period of rapid adjustment of the temperature profile whereby the temperature of droplets near the surface of the sheet falls more rapidly than the interior temperature. For optical depths between 0.5 and 4 and for emittances between 0.1 and 1 this adjustment was nearly complete at reduced time $\tilde{t} \sim 1$. After this adjustment period, although the absolute temperature decreased steadily with time, the relative temperature distribution $T(x)/T(x=S/2)$ remained nearly constant. This distribution was dependent, of course, on the optical depth and droplet emittance. The larger the optical depth the greater the fractional temperature decrease from the center to the edge of the sheet.

Figure 2 illustrates the magnitude of the temperature variations normal to the sheet. Plotted are curves showing the temperature (normalized to the temperature at the center of the sheet) as a function of optical distance from the center of the sheet, for combinations of (ϵ_0, τ_0) of $(0.8,1)$, $(0.2,2.5)$, and $(0.1,5)$, and for a time t^* at which the mean temperature has decreased to 0.8 of its iniital value T_0. These parameters are typical of those which might be used in a liquid droplet radiator,[3] and the profiles represent the temperature distribution at the droplet collector for an LDR designed so that the mean droplet temperature decreases by 20% during flight. For $\epsilon_0 = 0.1$, $\tau_0 = 5$, the surface temperature is 12% below the center temperature, and for the other cases the difference is 6-7%. Although these differences are substantial, considering that the fractional decrease in mean temperature is 20%, the effect on sheet emissivity is not large. This is illustrated in Fig. 3, which shows the emissivity of the sheet as a function of time, normalized to t^*. For an LDR these curves

correspond to sheet emissivity as a function of distance from the droplet generator to the droplet collector. For $\varepsilon_0=0.1$, $\tau_0=5$, the emissivity falls from 0.486 to 0.466, a fractional decrease of 4%, while for $\varepsilon_0=0.8$, $\tau_0=1$, the fractional decrease in ε_s is only ~2%. The assumption of a uniform temperature profile would, of course, yield a constant emissivity equal to the initial emissivity of the non-uniform temperature case.

We conclude that for values of ε_0 and τ_0 of interest for LDR applications, it is reasonably accurate to assume a constant emissivity of the droplet sheet, computed as though no temperature profile develops. Our earlier investigations[3] have shown that a reasonable compromise between minimizing the sheet area (larger optical depth) and minimizing sheet mass (smaller optical depth) would result from choosing $\tau_0 \simeq 0.5/\varepsilon_0$. This choice results in a sheet emissivity ($\varepsilon_s = 0.5\pm0.05$ for droplet emittances ε_0 betwen 0.05 and 1. The existence of a temperature profile may of course be critically important when the heat transfer medium operates close to the freezing point, in which case the droplets near the sheet surface may solidify. On the other hand, in cases where the fractional decrease in mean droplet temperature is small, a temperature profile may not have time to fully develop.

Effects of Non-Isotropic Scattering

As mentioned previously, to isolate the effects of non-isotropic scattering on droplet sheet emissivity, computations of this emissivity were made assuming a uniform temperature droplet sheet. Thus the source function $J_\nu^B(T)$ in the integrand of the integral equation for I_ν (eq. (8)) is time-independent, as is I_ν itself. Denoting the function in curly braces in eq. (8) by $\tilde{L}_\nu$ and defining a new dimensionless intensity function $L_\nu = \tilde{L}_\nu/\varepsilon_0 J_\nu^B(T)$, we obtain:

$$L_\nu(\tau_\nu,\theta) = 1 + \omega\int\limits_{0}^{\pi/2} d\theta'\sin\theta' \frac{1}{\cos\theta'} \tag{16}$$

$$+ \quad\quad \cdot \{ \gamma_\nu^+(\theta,\theta') \int\limits_{0}^{\tau} d\tau_\nu' \, L_\nu(\tau_\nu',\theta')\exp[-\frac{\tau_\nu-\tau_\nu'}{\cos\theta'}]$$

$$+ \gamma_\nu^-(\theta,\theta') \int\limits_{0}^{\tau_{0\nu}} d\tau_\nu' L_\nu(\tau_\nu',\theta)\exp[-\frac{\tau_{0\nu}-\tau_\nu-\tau_\nu'}{\cos\theta'}]\} \quad,$$

and the spectral sheet emissivit becomes:

$$\varepsilon_{S\nu} = 2\varepsilon_0 \int\limits_{0}^{\tau_{0\nu}} d\tau_\nu\int\limits_{0}^{\pi/2} d\theta \; s\mathrm{i} \ni L_\nu(\tau_\nu,\theta)\exp[-\frac{\tau_{0\nu}-\tau_\nu}{\cos\theta}] \quad. \tag{17}$$

Because of our assumption that t ⋅ optical properties of the droplet medium are frequency-independent, the s⎸ ⋅ctral variation of droplet sheet emissivity arises solely from the freq⎸ ncy (or z) dependence of Φ from which γ^+ and γ^- are computed.

In lieu of finding solutions of eq. (16) using Mie scattering phase functions to determine $\gamma^\pm$, a sim⎸ ier approach was used to find the magnitude of the effects of non-isotropic scattering on ε_S. We neglect the frequency dependence of Φ (or equivalently, simply solve eq. (24) at a single frequency) and represent Φ as a series of Legendre polynomials:

$$\Phi(\hat\Omega,\hat\Omega') = 1 + \sum_{\ell=1}^{N} P_\ell(\hat\Omega\cdot\hat\Omega')a_\ell$$

where the argument $\hat\Omega\cdot\hat\Omega'$ is the cosine of the angle η between incident and scattered light, and the leading term of unity ($a_0=1$) is required to insure that $\int d\Omega \, \Phi(\Omega,\Omega') = 4\pi$. The coefficients a_ℓ are chosen to represent various

types of scattering (isotropic, predominantly forward, predominantly backward, and perpendicular), and the droplet sheet emissivities corresponding to these scattering types are determined. This representation greatly reducs the computational complexity since the functions $\gamma^{\pm}$ can be evaluated analytically:

$$\gamma^{\pm}(\theta,\theta') = 2\pi \sum_{\ell=0}^{N} a_{\ell} P_{\ell}(\cos\theta) P_{\ell}(\pm\cos\theta').$$

In addition the intensity function L can be represented as a series of Legendre polynomials:

$$L(\tau,\mu) = L_0(\tau) + \sum_{\ell=1}^{N} L_{\ell}(\tau) P_{\ell}(\mu) a_{\ell}$$

where $\mu = \cos\theta$.

The components L_{ℓ} obey the relations:

$$L_0(\tau) = 1 + \frac{\omega}{2} \sum_{m=0}^{N} \int_0^1 \frac{d\mu}{\mu} P_m(\mu) \{ \int_0^{\tau} d\tau' L_m(\tau') \exp[-\frac{\tau-\tau'}{\mu}]$$

$$+ \int_0^{\tau_0-\tau} d\tau' L_m(\tau') \exp[-\frac{\tau_0-\tau-\tau'}{\mu}] \}$$

$$L_{\ell}(\tau) = 2\pi\omega \sum_{m=0}^{N} \int_0^1 \frac{d\mu}{\mu} P_{\ell}(\mu) P_m(\mu) \{ \int_0^{\tau} d\tau' L_m(\tau') \exp[-\frac{\tau-\tau'}{\mu}]$$

$$+ (-1)^{\ell} \int_0^{\tau_0-\tau} d\tau' L_m(\tau') \exp[-\frac{\tau_0-\tau-\tau'}{\mu}] \}$$

and the droplet sheet emissivity is:

$$\epsilon_S = 2\epsilon_0 \int_0^{\tau_0} \{L_0(\tau)E_1(\ \tau_0-\tau\ )$$

$$+ \sum_{\ell=1}^{N} a_\ell L_\ell(\tau) \int_0^1 d\mu P_\ell(\mu)\ \exp[-\frac{\tau_0-\tau}{\mu}\ ]\} \quad .$$

The integrals over μ can be evaluated immediately to yield a series of exponential integrals, since the functions $P_\ell(\mu)$ are simple polynomials of degree ℓ. One is left with a series of integral equations which are solved by discretizing the variable τ and solving the resulting set of linear equations by matrix inversion. The solutions are parameterized by the optical depth τ_0, the droplet emittance ϵ_0, and the coefficients $a_1,...,a_N$.

This solution procedure was carried out for values of ϵ_0 ranging from 0.1 to 1 and for optical depths ranging up to 4.0, with the following choices of coefficients:

$a_{\ell>1} = 0$ isotropic scattering

$a_1 = 1,\ a_{\ell>1} = 0$ forward scattering

$a_1 = -1,\ a_{\ell>1} = 0$ backward scattering

$a_2 = -1,\ a_{\ell\neq2} = 0$ $90°$ scattering

The isotropic scattering case corresponds to our previous results (Ref. 1). Figure 4 shows the dependence of droplet sheet emissivity on τ_0 and ϵ_0 for isotropic, forward and backward scattering. Forward scattering is seen to increase ϵ_S while backward scattering decreases ϵ_S, with respect to isotropic scattering. Emissivity values for $90°$ scattering were found to lie between the values for forward and backward scattering. For droplet sheets with the product $\epsilon_0\tau_0 \simeq 0.5$, non-isotropic scattering has a significant effect on sheet emissivity only at low droplet emittances ϵ_0. An emittance $\epsilon_0 = 0.1$ and an optical dpeth $\tau=5$ yields $\epsilon_S = 0.50$ for forward

scattering, ε_s = 0.44 for backward scattring, and ε_s = 0.46 for isotropic scattering. These calculations were only carried out to determine the maximum effects non-isotropic scattering might have on sheet emissivity. In fact, the variation of the angular scattering distribution with frequency makes the effect of non-isotropic scattering on sheet emissivity much less than for this "worst case" model.

References

1. A.T. Mattick and A. Hertzberg, "Liquid Droplet Radiators for Heat Rejection in Space," J. Energy 5, 387-393 (1981).

2. A.T. Mattick and A. Hertzberg, "The Liquid Droplet Radiator." Acta Astronautica 9, 165-177 (1982).

3. A.T. Mattick and A. Hertzberg, "Liquid droplet Radiator Technology Issues." First Symposium on Space Nuclear Power Systems, Albuquerque, NM, 11-13 Jan. 1984.
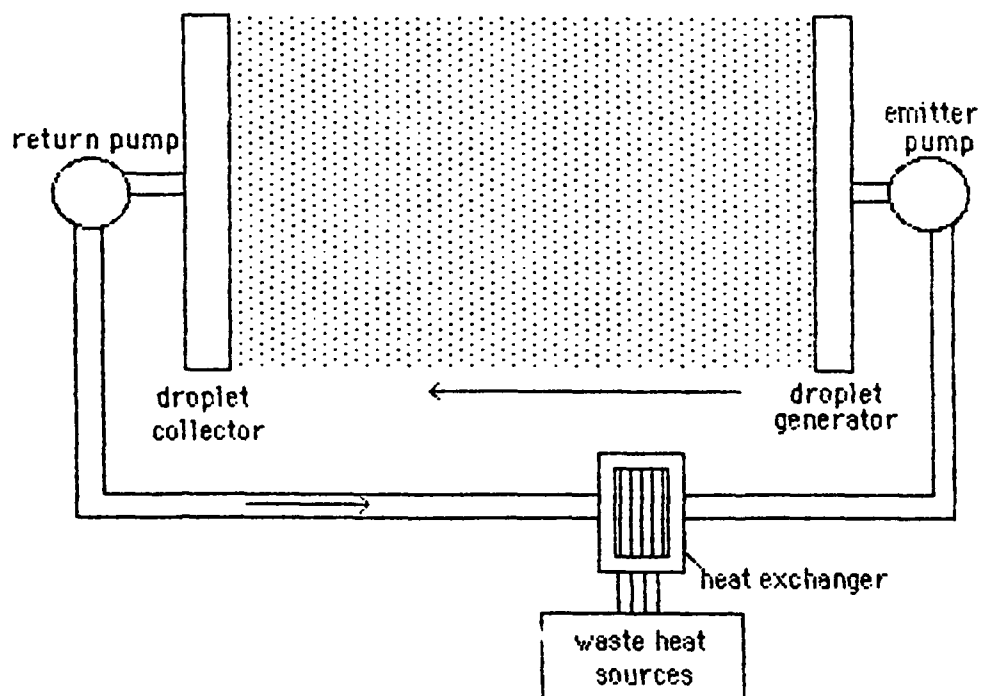
Fig.   1   Baseline configuration for the liquid
          droplet radiator.
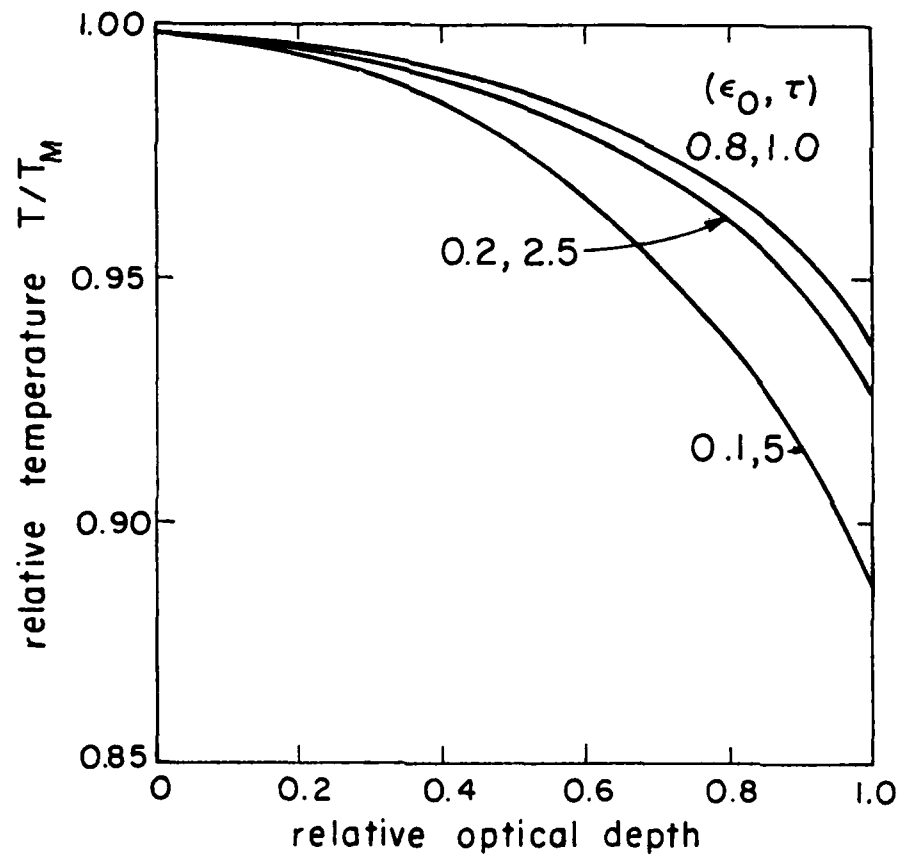
Fig. 2   Relative temperature profile in a droplet
          sheet which has cooled to a mean temperature
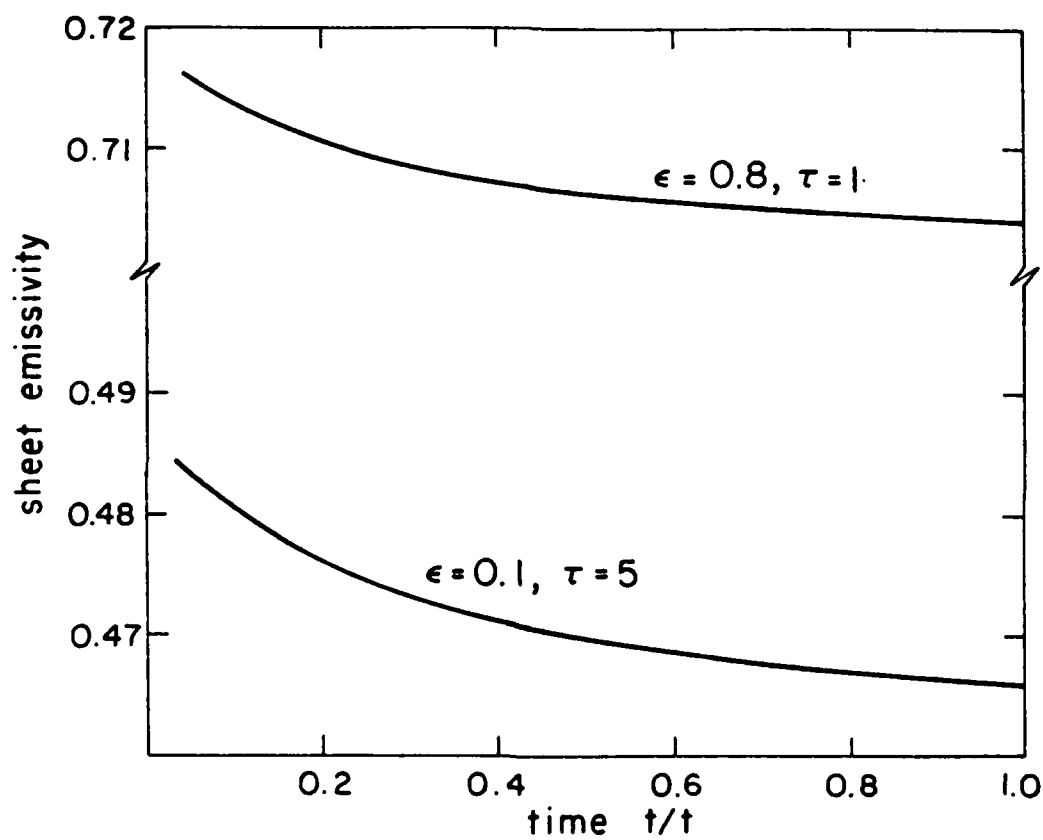   of 0.8 of the initial uniform temperature.

Fig. 3 Variation of droplet sheet emissivity with time due to development of a temperature profile normal to the sheet.
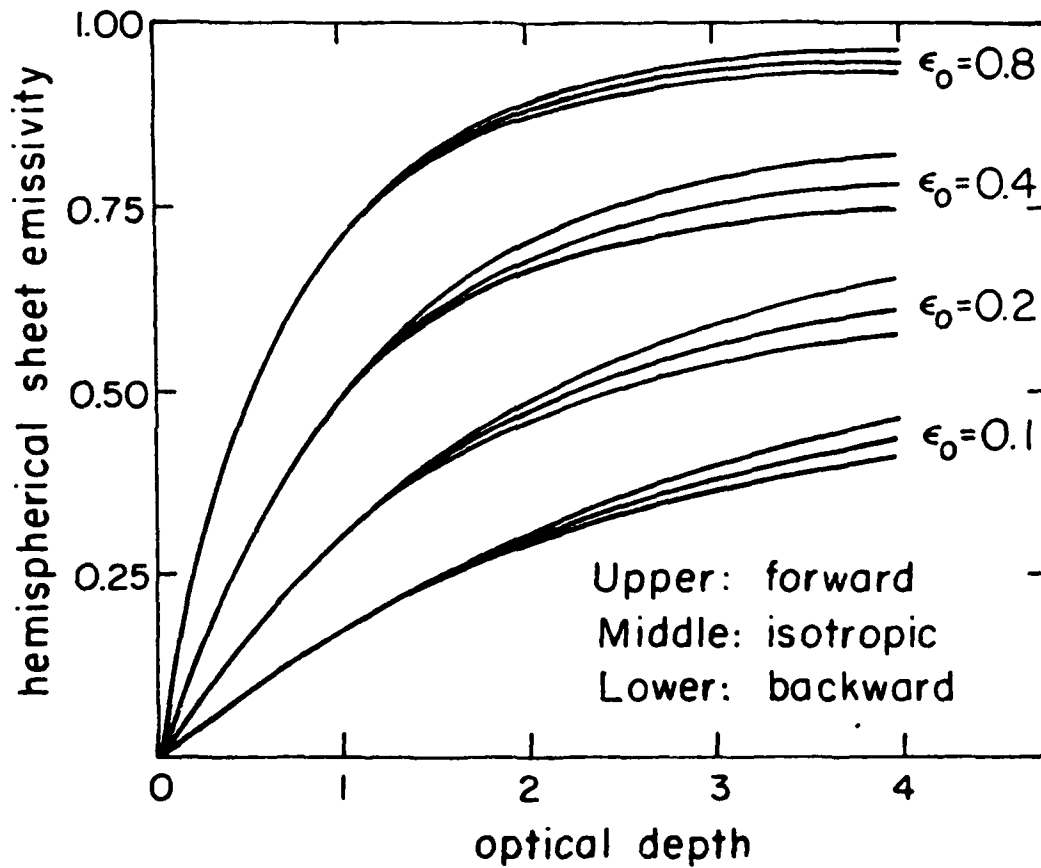
Fig. 4   Droplet sheet emittance vs optical depth for
          non-isotropic scattering (Legendre series approx.).

END

DTIC

9 — 86